# Calibration Methods and Results for Activity-Travel Scheduling Models

Xiao FU [a], William H.K. LAM [b], Yiliang XIONG [c]

[a,b,c] *Department of Civil and Environmental Engineering, The Hong Kong Polytechnic University, Hong Kong*
[a] *E-mail: xiao.fu@connect.polyu.hk*
[b] *E-mail: william.lam@polyu.edu.hk*
[c] *E-mail: wlxiong@gmail.com*

**Abstract**: This paper presents calibration methods for individual's and household's activity-travel scheduling models. Various model parameters are calibrated such as the parameters in marginal activity utility function and the coefficients of intra-household interactions. Numerical methods for solving the model calibration problem are optimized based on the mathematical property of the models. Hypothetical numerical experiments are conducted to generate time-series data for model calibration.

*Keywords*: Model Calibration, Maximum Likelihood Method, Marginal Utility Function

## 1. INTRODUCTION

To model the dynamics in activity scheduling, the series of decisions made by the traveller can be formulated as a Markov decision process (MDP) (Eckstein and Wolpin, 1989; Aguirregabiria and Mira, 2010). Previous applications of MDP in activity scheduling behaviour can be found in Jonsson and Karlström (2005) and Xiong (2013). The dependency of travellers' choices on their states can be investigated and the forward-looking behaviour in decision making can be considered by MDP model.

In the literature, the MDP model is traditionally estimated using Nested Fixed-Point (NFXP) algorithm (Rust, 1987, 1988). The NFXP algorithm finds the estimates in a nested manner. An inner fixed-point algorithm computes the unknown endogenous variables for each value of model parameter. In activity-travel scheduling models, the endogenous variables are the travellers' decisions over time. An outer hill climbing algorithm searches for the model parameter that maximizes the likelihood function. The NFXP algorithm is an intuitional and natural method of implementing the maximum likelihood method. The drawback is the computational burden of solving the dynamic programming problem thousands of times in the inner loop. Even though the original author implemented the algorithm in GAUSS programming language and the program is in the public domain, the code has not been updated for years. The researcher has to implement the algorithm from scratch if it is adopted to solve the calibration problem.

The above method is computational demanding and is thought to be impractical in many contexts. Formulating the calibration problem as Mathematical Programming with Equilibrium Constraints (MPEC) greatly reduce the computational burden (Su and Judd, 2012). Thus, MPEC approach is adopted in this study for solving the maximum likelihood problem.

The MPEC approach aims to search the model parameters and endogenous variables to maximize the likelihood function subject to equilibrium constraints. The endogenous variables fulfil the equilibrium condition defined by the model parameters. The researcher can simply write down the likelihood function and the equilibrium constraints in algebraic modelling languages. Then the model parameters are estimated with the state-of-the-art constrained nonlinear optimization solvers. The calibration of individual and household activity-travel scheduling models is implemented in A Mathematical Programming Language (AMPL) and solved with the software named KNITRO.

The NFXP algorithm solves the dynamic programming problem with high accuracy for each guess of the model parameters. In contrast, most modern solvers of MPEC only need to solve the dynamic programming problem at the final iteration for calculating the estimates. The computational burden is greatly reduced by this strategy. Su and Judd (2012) showed that if MPEC and NFXP are used to solve the same calibration problem, the two methods yield the same calibration results.

This study aims to use statistical methods for estimating the parameters of the individual's activity-travel scheduling MDP model proposed by Xiong and Lam (2011) and an extended household's MDP model. Time-series data are required for calibration of model parameters. The dataset should include travellers' activity choices and geographic locations over time. Due to the cost of collecting time-series activity-travel data, hypothetical numerical experiments are conducted in this study to generate the dataset.

The remainder of this paper is organized as follows. Section 2 illustrates the formulation of maximum likelihood method for the model calibration. Section 3 presents the data generated from numerical experiments and the calibration results of individual's activity-travel scheduling model. Section 4 presents the calibration of the household's activity-travel scheduling model. The final section summarizes the paper and concludes with a few suggestions for future research.

## 2. MAXIMUM LIKELIHOOD METHOD

MDP models can be categorized into two main groups based on how the time is modelled: the discrete-time MDP and the continuous-time MDP. In discrete-time MDP model, the planning horizon is divided into equal periods. It is reasonable to assume that the traveller takes activity-travel choices at discrete decision epochs and thus, discrete-time MDP model is adopted in this paper.

The state of individual $i$ at time $t$, $s_{it}$, includes a set of variables that provide all the information for making decision at time $t$. From a researcher's point of view, we can partition the state into two subvectors: $s_{it} = (x_{it}, \varepsilon)$, where $x_{it}$ is the observable part of the state, and the unobservable state ε is the source of variations in the MDP model.

Rust (1994) proposed a unified framework for structural estimation of MDP model. The contribution of individual $i$ to the log-likelihood function is expressed as follows:

$$\log l_i(\eta) = \sum_{t=1}^{T_i} \log P\left(d_{it} \mid s_{it}, \eta\right) + \sum_{t=1}^{T_i-1} \log p\left(s_{i,t+1} \mid d_{it}, x_{it}, \eta\right) + \log P\left(s_{i1} \mid \eta\right) \quad (1)$$

where $\eta$ represents the vector of model parameters; $d_{it}$ denotes the observed decision of individual $i$ at time $t$; $p\left(s_{i,t+1} \mid d_{it}, x_{it}, \eta\right)$ is the state transition probability function conditional on $d_{it}, x_{it}$ and $\eta$.

Assuming that $\varepsilon$ is normally distributed with *N*×*M*-variate probability density function $G_\varepsilon(\cdot)$, the probability of observing choice $d_i$ can be calculated by integrating over all possible values of $\varepsilon$:

$$P(d_{it} \mid \eta) = \int \cdots \int G_\varepsilon(\varepsilon) d\varepsilon \tag{2}$$

If the choice is independent over individuals, the likelihood of all individuals' activity choices can be expressed as the product of each individual's activity choice probability:

$$L(d_1, \ldots, d_I \mid \eta) = \prod_{i=1}^{I} l_i(\eta) \tag{3}$$

As the choice probability involves multi-dimensional integral, Equation (3) is evaluated using the GHK simulator. Consistent estimates can be obtained by the simulated likelihood method.

## 3. CALIBRATING INDIVIDUAL'S ACTIVITY-TRAVEL SCHEDULING MODEL

The calibration of the parameters in individual's activity-travel scheduling MDP model (refer to (Xiong and Lam, 2011)) is presented in this section. With a given set of parameters, Monte Carlo experiments were conducted to generate time-series data. Based on the generated data, MPEC approach was employed to calibrate the model parameters. The difference of the actual parameters and the estimated parameters was used to evaluate the accuracy of the calibration method.

### 3.1 Marginal Utility Functions

It is believed that various activity participations have different preferred times. Activity participation usually starts with a warming up phase in which the marginal activity utility increases. After reaching a maximum point, the marginal utility decreases. Two marginal utility functions are introduced in this paper. The first one is a bell-shaped function proposed by Ettema and Timmermans (2003):

$$g_a(t) = \frac{\gamma_a \lambda_a U_a^{\max}}{\exp\left[\gamma_a (t - \xi_a)\right] \cdot \left\{1 + \exp\left[-\gamma_a (t - \xi_a)\right]\right\}^{\lambda_a + 1}} \tag{4}$$

where $g_a(t)$ denotes the marginal utility of performing activity $a$ at time $t$; $U_a^{\max}$ is the maximum marginal utility; $\gamma_a$, $\lambda_a$, and $\xi_a$ are parameters to be calibrated.

The second marginal utility function is based on a scaled probability density function of the scaled Cauchy distribution (Ettema *et al*., 2004):

$$g_a(t) = \frac{U_a^{\max}}{\pi c_a \left[1 + \left(\frac{t - b_a}{c_a}\right)^2\right]} \tag{5}$$

where $U_a^{\max}$ is the maximum marginal utility; $b_a$ is the time at which the marginal utility reaches the maximum value and $c_a$ determines the period in which a satisfactory marginal utility can be obtained.

Figure 1 depicts the temporal profiles of the two marginal utility functions. The peak of each curve shows the time at which the marginal utility reaches the maximum value. Both functions are unimodal (having a single local maximum) and ensure that the marginal activity utility increases in the warm-up period and decreases in the saturated period. Although the shapes of the two curves are similar, the scaled Cauchy distribution has a sharp peak and a long tail. Essentially, either marginal utility function can be adopted for empirical analysis. However, the scaled Cauchy distribution has fewer parameters and a simpler functional form. Thus, the scaled Cauchy distribution has fewer problems on identifiability and it is employed in the following numerical experiments.

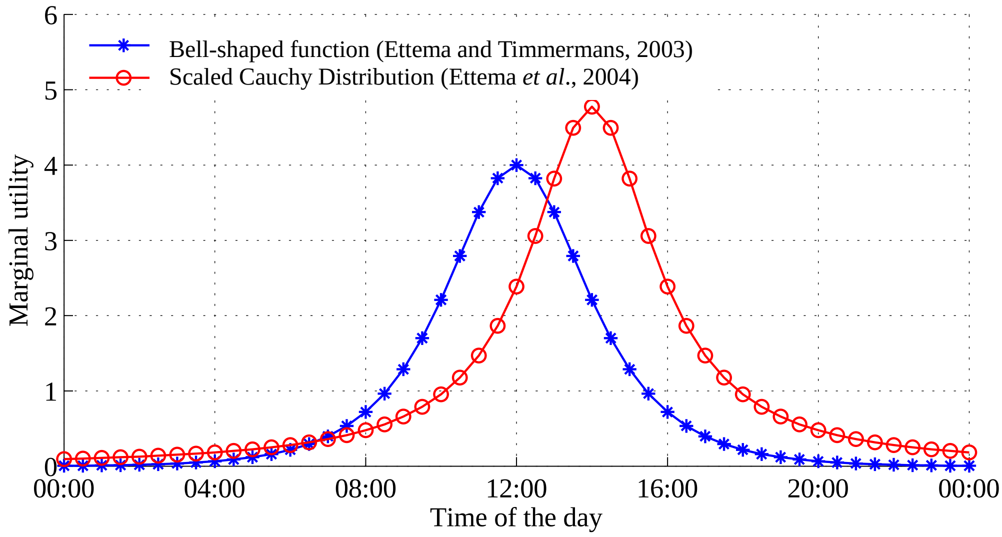

Figure 1. Temporal profiles of two types of marginal utility function

### 3.2 Activity-Travel Data Generation

Figure 2 shows a transport network with 3 nodes. Each node represents an activity location. The free flow travel time of each link is given in the figure. The travel time considering congestion effect is captured by a BPR function:

$$t_l\left(f_l\left(t\right)\right)=t_l^0\times\left(1+0.15\left(\frac{f_l\left(t\right)}{5000}\right)^4\right) \tag{6}$$

where $t_l^0$ is the free flow travel time and $f_l\left(t\right)$ is the flow on link $l$ at time $t$.

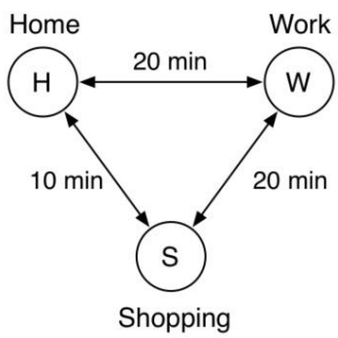

Figure 2. A 3-node transport network

The time is evenly divided into 5-minute intervals. The value of time is set to 60. The discount ratio of the future utility is set to 0.95. These two parameters are treated as fixed and known to maintain the identifiability.

The marginal activity utility varies over time and is defined by marginal utility function Equation (5). Table 1 presents the actual values of the parameters in marginal utility function. The parameters are explained in Section 3.1. They are to be estimated. The estimated values will be compared with the actual values in the following.

Table 1. Parameters in marginal utility function

| Activity types | Parameters | | | | | |
|---|---|---|---|---|---|---|
| *Home* | $U_1^{\max}$ | 3600 | $b_1$ | 0 | $c_1$ | 320 |
| *Work* | $U_2^{\max}$ | 2500 | $b_2$ | 840 | $c_2$ | 180 |
| *Shopping* | $U_3^{\max}$ | 2000 | $b_3$ | 1140 | $c_3$ | 210 |

Figure 3 depicts the shape of the marginal utility function. There are two in-home activities: *Home-AM* and *Home-PM*. It is assumed that people receive maximum utility of *Home* activity at 00:00, so the parameters in the marginal utility functions of *Home-AM* and *Home-PM* are the same as shown in Table 1. Before noon, the utility of *Home-AM* gives the utility of *Home.* After noon, the utility of *Home-PM* gives the utility of *Home.* From Figure 3, it can be found that, from 00:00 to 08:00, *Home-AM* is the activity with the maximum marginal utility. From 08:00 to 17:00, *Work* dominates the other activities in terms of marginal utility. From 17:00 to 21:00, *Shopping* is the dominate activity. From 21:00 to midnight, *Home-PM* is the dominate activity.

In this paper, the day-to-day dynamic is not considered. A potential extension of the individual and household MDP models is to consider day-to-day dynamic in activity-travel scheduling. The effect of certain activities can persist for multiple days and thus the activities participated in one particular day can influence the later activity-travel schedules (Arentze and Timmermans, 2009). For example, the goods purchased during a shopping trip can be adequate for a few days' usage. The probability of making another shopping trip on the next day will be very low. Another point to note is that activity-travel schedules on weekdays and weekends differ significantly. Compulsory activities, such as work and school are regular occurrences on weekdays, while some non-compulsory activities, such as physical exercise, are usually performed at the weekend.

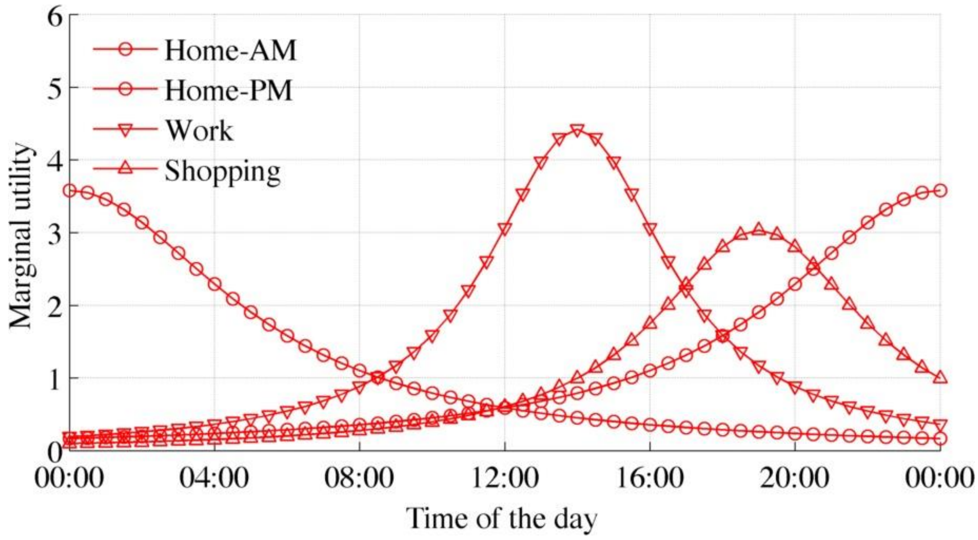

Figure 3. Temporal profile of the marginal utility function

Travellers are assumed to choose the daily activity program, activity duration and departure time to maximize the overall utility of the entire day. Their utility maximization behaviours are described by the MDP model (Xiong and Lam, 2011). Under these assumptions, time-series data for 288 time intervals (24 hours) and 10,000 travellers were generated in the numerical experiment. The choice probability is assumed to follow Equation (21) in Xiong and Lam (2011) and the parameter $\theta$ is 0.2.

The Monte Carlo method was conducted as follows: (1) fix the model parameters at actual values and solve the Bellman equation (refer to Equation (17) in Xiong and Lam (2011)) to obtain the optimal value of $\overline{V}(s), s \in S$; (2) use the actual values of the model parameters and $\overline{V}(s)$ to compute the conditional choice probability (refer to Equation (19) in Xiong and Lam (2011)); (3) generate choices and state transitions for 10,000 travellers in 288 periods based on the choice probability and the travel time.

### 3.3 Calibration Results

Before reporting the calibration results, the profile of log-likelihood function and the maximum values are illustrated and discussed. Given the activity-travel data, the log-likelihood function depends on a vector of parameters. It is difficult to visualize a multidimensional function. This section thus seeks to illustrate the impact of one or two parameters of interest on the log-likelihood function.

The parameters of marginal utility function can be represented as a vector, $\eta = \left(U^{\max}, b, c\right)$, where $U^{\max} = \left(U_1^{\max}, U_2^{\max}, U_3^{\max}\right)$, $b = \left(b_1, b_2, b_3\right)$, $c = \left(c_1, c_2, c_3\right)$. Denote $\eta$ as the overall maximum likelihood estimate of $\eta$ and let $\eta\left(b_2\right)$ be the vector of parameters with all the parameters except $b_2$ fixed at the maximum likelihood estimate of $\eta$. Then the log-likelihood function is defined by:

$$l_i\left(b_2\right) = l_i\left(\eta\left(b_2\right)\right) \tag{7}$$

Figure 4 illustrates the log-likelihood $l_i\left(b_2\right)$ as a function of $b_2$ with other parameters fixed at the estimated values. The log-likelihood function $l_i\left(b_2\right)$ is non-convex and has a unique maximum value at $b_2 = 841.4$, which is very close the true value 840. If $b_2$ is shifted a little from the optimal value, the value of the log-likelihood changes dramatically. Vector $b$ determines the time at which the marginal utility function reaches the maximum value and thus, has a strong influence on the activity time choice.

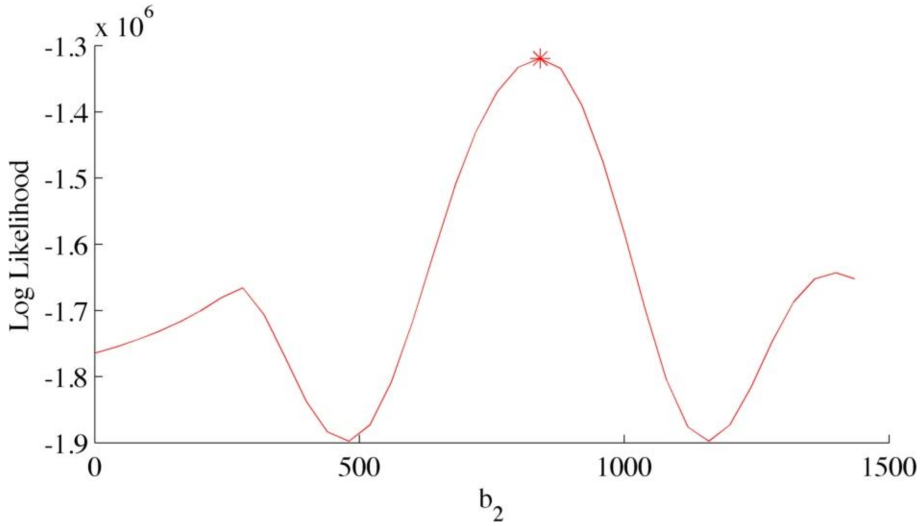


Figure 4. The log-likelihood function $l_i$ ($b_2$)

Let $\eta(b_2, b_3)$ be the vector of parameters with all the parameters except $b_2$ and $b_3$ fixed at the maximum likelihood estimate of $\eta$. The log-likelihood function is defined as

$$l_i(b_2, b_3) = l_i\left(\eta(b_2, b_3)\right) \tag{8}$$

Figure 5 depicts the log likelihood as a function of $b_2$ and $b_3$. The overall appearance of the log-likelihood function reveals a rather complicated relationship between the log likelihood and the model parameters $b_2$ and $b_3$. Multiple local optimal solutions can be found in the figure.

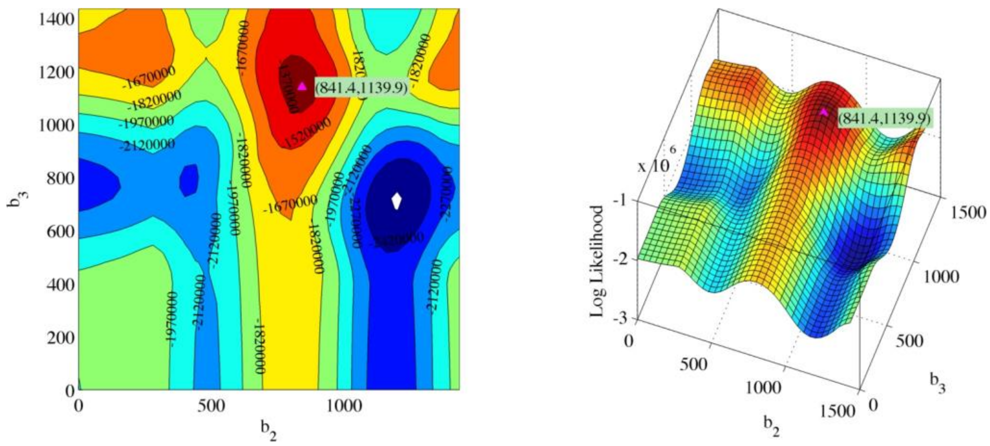


Figure 5. Contour and 3-D plot of the log-likelihood function $l_i$ ($b_2$, $b_3$)

Table 2 presents the maximum likelihood estimates of the model parameters. In general, the relative errors of the estimates are within 10%. The estimate of maximum marginal utility $U^{max}$ is smaller than the actual value. The estimates of the location parameter $b$ are very close to the actual values. The location parameter $b$ has a greater impact on the dominate period of each activity than $U^{\max}$ and thus to a great extent determines the activity choice probability and the log-likelihood. This is the reason why the estimates of $b$ are more accurate than that of $U^{\max}$. Similarly, the same argument applies to the estimates of $c$, which determines the width of the marginal utility curve.

Table 2. The estimates of parameters in marginal utility function

| Parameters | $U^{\max}$ | | | $\hat{b}$ | | | $\hat{c}$ | | |
|---|---|---|---|---|---|---|---|---|---|
| Activity types | *Home* | *Work* | *Shopping* | *Home* | *Work* | *Shopping* | *Home* | *Work* | *Shopping* |
| Actual values | 3600 | 2500 | 2000 | 0 | 840 | 1140 | 320 | 180 | 210 |
| Estimated values | 3517 | 2481 | 2051 | 0 | 841 | 1140 | 305 | 168 | 219 |

## 4. CALIBRATING HOUSEHOLD'S ACTIVITY-TRAVEL SCHEDULING MODEL

This section presents the calibration of the household's activity-travel scheduling MDP model (refer to (Xiong, 2013)). Two types of parameters are calibrated, i.e. the intra-household interaction coefficients and the parameters in marginal utility function. Household members have distinct preference over the timing of activities and thus, the parameters in marginal utility function for each member are estimated.

### 4.1 Household Activity-Travel Data Generation

Figure 6 shows a 4-node road network on which activity-travel decisions are made. There are 10,000 behaviourally homogeneous households and each household is composed of two adults: Individual 1 and Individual 2. Node H represents the residential location. Node W1 and W2 are the workplaces of the household members respectively. For simplicity, travel time is assumed deterministic and the congestion effect is captured by a BPR function,

$$\tau_l\left(f_l(t)\right) = t_l^0 \times \left(1 + 0.15\left(\frac{f_l(t)}{5000}\right)^4\right) \tag{9}$$

where $f_l(t)$ is the flow on link $l$ at time $t$. The equivalent disutility of travelling for one hour is $\alpha = 60$. The discount ratio of the future utility is set to $\beta = 0.95$. The entire day (24 hours) is divided into 288 periods with 5-minute per period.

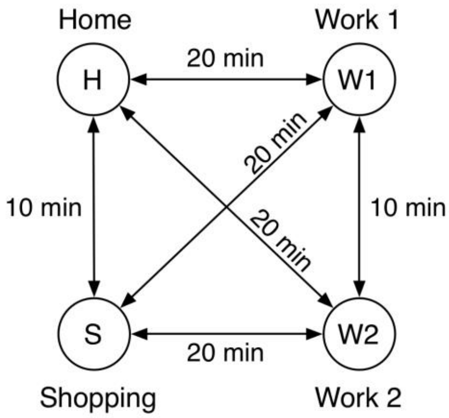


Figure 6. A 4-node road network

The scaled Cauchy distribution is adopted as the marginal utility function in this example. Three types of activity are considered in the example: *Home*, *Work*, and *Shopping*. The parameters of utility function for each activity are presented in Table 3. The two household members have distinct preferences for work and shopping activity. Individual 1 is more willing to go shopping than Individual 2, but receives less utility from work (represented by the bold values in Table 3). Figure 7 depicts the temporal profiles of the individual's marginal activity utility functions.

Table 3. Parameters of marginal utility functions for the household

| Activity | Parameters of utility function | | | | | |
|---|---|---|---|---|---|---|
| | Individual 1 | | | Individual 2 | | |
| | $U^{max}$ | $b$ | $c$ | $U^{max}$ | $b$ | $c$ |
| *Home* | 3600 | 0 | 320 | 3600 | 0 | 320 |
| *Work* | **2500** | 840 | 180 | **3000** | 840 | 180 |
| *Shopping* | **2000** | 1140 | 210 | **1500** | 1140 | 210 |

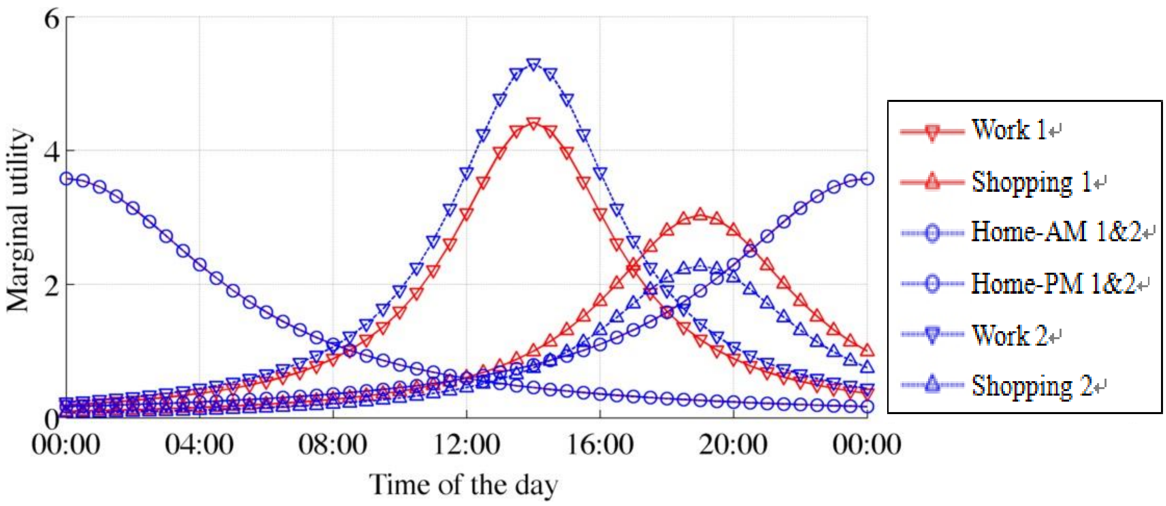


Figure 7. Temporal profile of the marginal utility function

The marginal utility for a household is defined as

$$r_a = \sigma_1 \cdot r_{1,a} + \sigma_2 \cdot r_{2,a} + \rho_a \cdot r_{1,a} \cdot r_{2,a} \tag{10}$$

where $r_{i,a}$ is the individual utility that household member $i$ can obtain when pursuing the activity $a$ independently. The welfare of the individuals in a household is treated equally important. The weight parameter $\sigma_i$, representing the relative influence of household member $i$, is thus fixed at the same value, $\sigma_1 = \sigma_2 = 1.0$. The interaction coefficient *Work* $\rho_2$ is set to zero. The interaction coefficients of *Home* and *Shopping* are set as $\rho_1 = 0.3$ and $\rho_3 = 0.2$.

### 4.2 Calibration Results

The main focus of this section is to show how to estimate the intra-household interaction coefficient $\rho$. The log-likelihood function is a multidimensional function of a vector of parameters and hard to be visualized. Following the approach presented in Section 3.3, the impact of one or two parameters of interest, i.e., the interaction coefficients, on log-likelihood function is visualized and discussed.

The parameters of the household's MDP model can be represented as a vector, $\eta = \left(U_1^{\max}, b_1, c_1, U_2^{\max}, b_2, c_2, \rho\right)$, where $U_i^{\max}$, $b_i$ and $c_i$ are the vectors of parameters defined for household member $i$'s marginal utility function, and $\rho$ is the vector of intra-household interaction coefficients defined for *Home*, *Work*, and *Shopping*, $\rho = (\rho_1, \rho_2, \rho_3)$.

Denote by $\eta$ the overall maximum likelihood estimate of $\eta$ and let $\eta(\rho_3)$ be the vector of parameters with all the parameters except $\rho_3$ fixed at the maximum likelihood estimate of $\eta$. Then the log-likelihood function is defined by:

$$l_i(\rho_3) = l_i\left(\eta(\rho_3)\right) \tag{11}$$

Figure 8 illustrates the log likelihood as a function of $\rho_3$ with other parameters fixed at the estimated values. The only local maximum of log-likelihood function $l_i(\rho_3)$ is also a global maximum. $l_i(\rho_3)$ has the global maximum at $\rho_3 = 0.188$. The figure shows that log-likelihood function $l_i(\rho_3)$ is concave in interval $[0,1]$. However, no formal proof is obtained to confirm this observation.

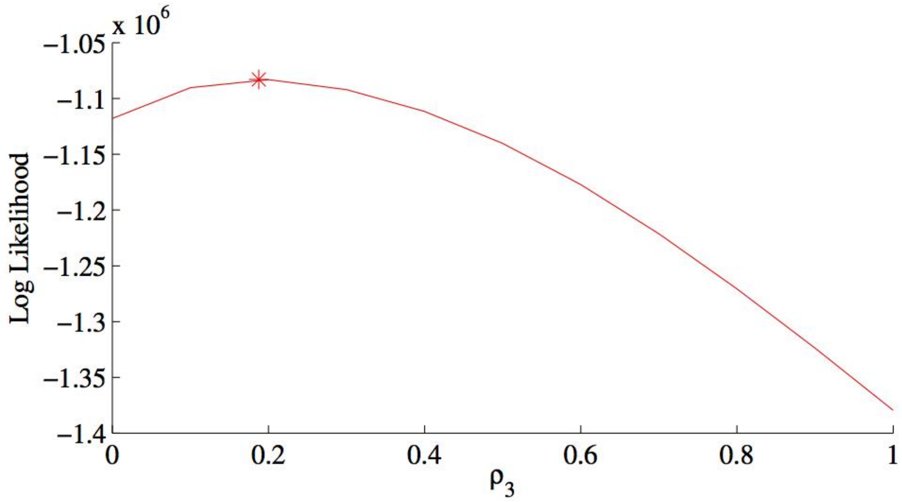


Figure 8. The log-likelihood function $l_i(\rho_3)$

Similarly, given the activity-travel data, the log-likelihood can be defined as a function of $\rho_1$ and $\rho_3$, i.e., $l_i(\rho_1, \rho_3)$. Figure 9 shows that the log-likelihood function $l_i(\rho_1, \rho_3)$ is concave in the unit square $[0,1]^2$ and has a global maximum at point $(\rho_1, \rho_3) = (0.282, 0.188)$.

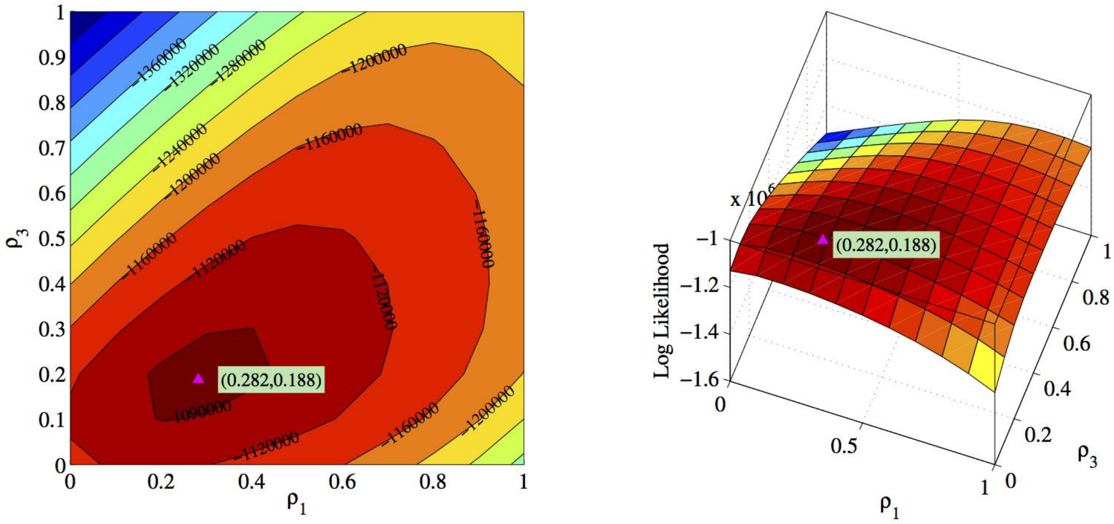


Figure 9. Contour and 3-D plot of the log-likelihood function $l_i(\rho_1, \rho_3)$

The true value of intra-household interaction coefficient $\rho$ is $(0.3, 0.0, 0.2)$ and the estimate of $\rho$ is $(0.282, 0.011, 0.188)$. The accurate calibration of $\rho$ can be contributed to the concaveness of the log-likelihood function over the unit cube $[0,1]^3$. Table 4 presents the maximum likelihood estimates of the parameters in marginal utility functions.

The household utility function (i.e. Equation (10)) is symmetric with respect to individual's utilities $r_{1,3}$ and $r_{2,3}$. Therefore, the respective estimates of $U_{1,3}^{\max}$ and $U_{2,3}^{\max}$ have little effect on the household utility as long as their product is comparable to that of the true values. As shown in Table 4, the estimates of $U_{1,3}^{\max}$ and $U_{2,3}^{\max}$ are 1791 and 1757, and their product is 3,146,787. The true values of $U_{1,3}^{\max}$ and $U_{2,3}^{\max}$ are 2000 and 1500 and their product is 3,000,000. This explains the imprecise calibration of these two parameters. The relative errors of the other estimates are within 10%.

Table 4. The estimates of parameters of the marginal utility functions for the household

| Household members | Parameters | $U^{\max}$ | | | $\hat{b}$ | | | $\hat{c}$ | | |
|---|---|---|---|---|---|---|---|---|---|---|
| | Activity types | *Home* | *Work* | *Shopping* | *Home* | *Work* | *Shopping* | *Home* | *Work* | *Shopping* |
| Individual 1 | Actual values | 3600 | 2500 | 2000 | 0 | 840 | 1140 | 320 | 180 | 210 |
| | Estimated values | 3654 | 2389 | 1791 | 1 | 828 | 1149 | 338 | 178 | 196 |
| Individual 2 | Actual values | 3600 | 3000 | 1500 | 0 | 840 | 1140 | 320 | 180 | 210 |
| | Estimated values | 3667 | 3114 | 1757 | 0 | 849 | 1128 | 305 | 182 | 226 |

## 5. CONCLUSIONS

In this study, maximum likelihood method is employed to calibrate the marginal activity utility function and intra-household interaction coefficient in activity-travel scheduling models. The calibration method requires observations of household members' activity-travel decisions over time episodes. The activity-travel data required for calibration were generated from numerical experiments. The calibration method was tested and evaluated with these hypothetical data.

Numerical methods were formulated and implemented to calibrate the activity-travel scheduling models. The calibration results were found satisfactory and the relative errors of most estimates were within 10%. Numerical experiments showed that the log-likelihood function was concave over the domain of intra-household interaction coefficient. This property enables efficient and accurate calibration of the interaction coefficient. In further research, travellers' activity-travel choices and geographic locations in a period should be collected for calibrating the activity-travel scheduling models.

## ACKNOWLEDGEMENTS

This work was jointly supported by a Postgraduate Studentship and a research grant from the Research Grant Council of the Hong Kong Special Administrative Region to the Hong Kong Polytechnic University (Project No. PolyU 5181/13E).

## REFERENCES

Aguirregabiria, V., Mira, P. (2010) Dynamic discrete choice structural models: A survey. *Journal of Econometrics*, 156(1), 38-67.

Arentze, T.A., Timmermans, H.J.P.. (2009) A need-based model of multi-day, multi-person activity generation. Transportation Research Part B: Methodology, 43, 251-265.

Eckstein, Z., Wolpin, K.I. (1989) The specification and estimation of dynamic stochastic discrete choice models: A survey. *The Journal of Human Resources*, 24(4), 562-598.

Ettema, D., Timmermans, H.J.P. (2003) Modeling departure time choice in the context of activity scheduling behaviour. *Transportation Research Record: Journal of the Transportation Research Board*, 1831, 39-46.

Ettema, D., Ashiru, O., Polak, J. (2004) Modeling timing and duration of activities and trips in response to road-pricing policies. *Transportation Research Record: Journal of the Transportation Research Board*, 1894, 1-10.

Ettema, D., Timmermans, H.J.P. (2003) Modeling departure time choice in the context of activity scheduling behavior. *Transportation Research Record: Journal of the Transportation Research Board*, 1831, 39-46.

Jonsson, R.D., Karlström, A. (2005) SCAPES - a dynamic microeconomic model of activity scheduling. In: European Transport Conference.

Rust, J. (1987) Optimal replacement of GMC bus engines: An empirical model of harold zurcher. *Econometrica* 55, 999-1033.

Rust, J. (1988) Maximum likelihood estimation of discrete control processes. *SIAM Journal on Control and Optimization*, 26, 1-19.

Rust, J. (1994) Structural estimation of markov decision processes. *Handbook of Econmetrics*, 4, 3081-3143.

Su, C.L., Judd, K.L. (2012) Constrainted optimization approaches to estimation of structural models. *Econometrica*, 80(5), 2213-2230.

Xiong Y.L. (2013) Modelling individual and household activity-travel scheduling behaviours in stochastic transportation networks. MPhil thesis. The Hong Kong Polytechnic University.

Xiong Y.L., Lam, W.H.K. (2011) Modelling within-day dynamics in activity scheduling: A markov decision process approach. *Journal of the Eastern Asia Society for Transportation Studies*, 9, 452-467.

Zheng, Y., Xie, X., Ma, W.Y. (2010) GeoLife: A collaborative social networking service among user, location and trajectory. *IEEE Data(base) Engineering Bulletin*, 33, 32-40.